6th International Conference on Advances in Experimental Structural Engineering
11th International Workshop on Advanced Smart Materials and Smart Structures Technology
August 1-2, 2015, University of Illinois, Urbana-Champaign, United States

Finite Element Model Updating of a 4-Story Reinforced Concrete Base-Isolated Building Tested at the E-Defense Shaking Table Facility

W.M. Elhaddad[1], P.T. Brewick[2], J.B. Hernandez[3], E.A. Johnson[4], E. Sato[5], T. Sasaki[6]

1 *Ph.D. Candidate, Sonny Astani Department of Civil and Environmental Engineering, University of Southern California, United States. E-mail: welhadda@usc.edu*

2 *Post doctoral Fellow, Sonny Astani Department of Civil and Environmental Engineering, University of Southern California, United States. E-mail: pbrewick@usc.edu*

3 *M.Sc. Student, Sonny Astani Department of Civil and Environmental Engineering, University of Southern California, United States. E-mail: barriosh@usc.edu*

4 *Professor, Sonny Astani Department of Civil and Environmental Engineering, University of Southern California, United States. E-mail: johnsone@usc.edu*

5 *Senior Researcher, National Research Institute for Earth Science and Disaster Prevention, 1501-21 Nishikameya, Mitsuta Shijimi-cho Miki, Hyogo, Japan 673-0515. E-mail: eiji@bosai.go.jp*

6 *Senior Researcher, National Research Institute for Earth Science and Disaster Prevention, 1501-21 Nishikameya, Mitsuta Shijimi-cho Miki, Hyogo, Japan 673-0515. E-mail: tomo_s@bosai.go.jp*

ABSTRACT

This paper develops and updates a finite element model of a base-isolated reinforced concrete building that was tested at Japan's E-Defense earthquake engineering research center in 2013 to evaluate the effects of seismic moat wall pounding and isolation during long-period earthquakes. This full-scale four-story moment frame building, with two reinforced concrete walls, sits on an isolation composed of rubber bearings, elastic sliders, U-shaped steel dampers and oil dampers. Designing controllable dampers for planned 2016 or 2017 tests requires a calibrated numerical model. The authors previously reported modal analysis results, based on random excitation responses during the 2013 tests. Herein, a finite element model (FEM) is developed and updated to match the identified modal parameters. The superstructure FEM consists of line and shell elements and (linear) spring isolation elements, resulting in 1757 nodes and 10,542 degrees of freedom. 21 parameters (various Young's moduli, isolation layer stiffnesses, and point masses) were updated iteratively using the Nelder-Mead simplex method using frequency residuals and mode shape MAC values between FEM modes and those identified from the 2013 random tests. The optimization converges to an updated FEM that provides much better match with the experimental data, reducing the frequency and MAC residuals by 60-90%.

KEYWORDS: *Model Updating, Shake Table Testing, Base Isolation, Nelder-Mead optimization.*

1. INTRODUCTION

Japan's Hyogo Earthquake Engineering Research Center, commonly called *E-Defense*, is a shake table testing facility constructed in the early 2000s in Miki City, Japan, for performing full-scale earthquake experiments to better understand the seismic behavior of building structures. The 20 m × 15 m shake table is capable of shaking test specimens in 6 degrees-of-freedom, thereby producing velocities of up to ±2 m/s and displacements of ±1m. For instance, a three-story self-centering rocking steel frames structure was tested in 2009 [1] to demonstrate the effectiveness of steel rocking frames with replaceable energy dissipating devices [2]. Other examples of such studies are earthquake loading experiments carried out on a 5-story steel moment frame building [3]; in these experiments, the structure was tested both in a fixed-base configuration and a base-isolated configuration using triple friction pendulum bearings and lead rubber bearings. These tests also aimed at understanding the behaviors of non-structural components, such as ceilings, piping systems and non-structural walls [3].

2. BACKGROUND

More recently, in 2013, a series of seismic shaking experiments were performed on a four-story base-isolated reinforced concrete (RC) building, shown in Figure 2.1(a) [4]. The structure is supported against lateral loads using RC moment frames along with two structural walls in one corner of the building. The building is base isolated using four different kinds of passive isolation and damping devices: rubber bearings, elastic sliding bearings, U-shaped steel dampers and oil dampers. In 2013, the building was subjected to a series of earthquake records to evaluate the effectiveness of the passive isolation, particularly with regard to pounding against the

seismic moat [4]. Additional tests using controllable passive dampers are planned for 2016 or 2017. It is essential to obtain a validated numerical model of the building in order to design the necessary control strategies that will be used in future tests.

The building was equipped with different types of sensors, including 42 accelerometers for measuring structural accelerations, denoted SA01X – SA14Z (Figure 2.2), 58 sensors for measuring forces in the isolators and 4 sensors for measuring displacements in the isolation layer. The structure was subjected to well-known earthquake records scaled to different magnitudes and applied in different directions. At the beginning of the first day of testing, and subsequently in between different earthquake records, a series of shaking table tests using random excitations in different directions were performed to calibrate and evaluate the extent of damage, in both the structure and the isolators.
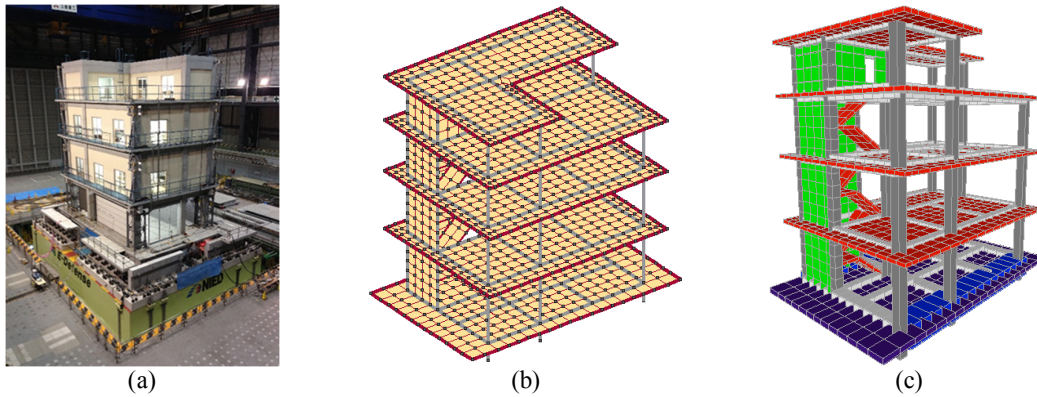

(a) (b) (c)

Figure 2.1 The base-isolated building specimen: (a) photo at the E-Defense testing facility; (b) FEM (discretized view); (c) FEM (extruded view)
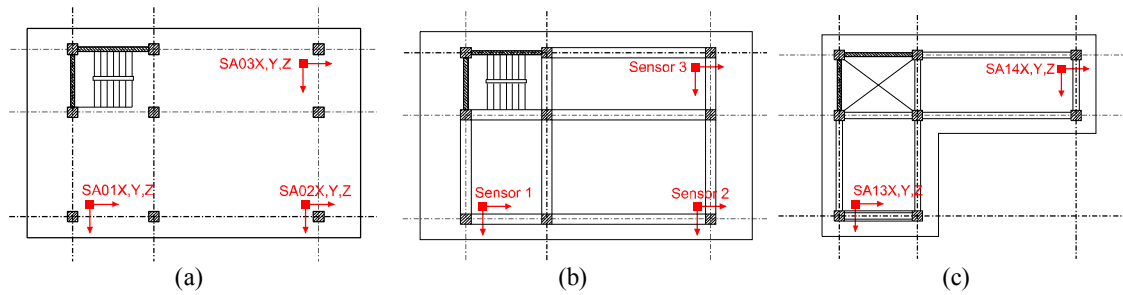

(a) (b) (c)

Figure 2.2 Schematic diagrams of the floor plans [5] showing locations of accelerometers used in the superstructure: (a) 1st floor; (b) typical floors; (c) roof

A previous study by the authors [6], reported modal analysis results, based on the 2013 initial tests with random excitations, using stochastic subspace identification (SSID) methods to obtain a set of stable mode shapes and natural frequencies. In that study, two SSID algorithms were used and their results were compared for validation. Specifically, the Numerical Algorithm for Subspace State-space System Identification (N4SID) [7] and the Enhanced Canonical Correlation Analysis (ECCA) [8] were chosen. The results of that study are summarized in Table 2.1 herein, as they represent the target mode shapes and frequencies for the model updating procedure presented subsequently. It is essential to note here the coupling between modes 1 and 2, because the identified frequencies are very close. If these two modal frequencies matched exactly, then their mode shapes are no longer unique, and a system identification would identify one pair of an infinite number of valid mode pairs on a two-dimensional manifold. This may pose a challenge for the model updating problem.

In this study, a numerical finite element model (FEM) is developed and updated to match the identified modal parameters. A FEM was developed for the base-isolated building as shown in Figure 2.1(b and c). The model includes the columns, beams, stairs, floors and structural walls. The resulting FEM is comprised of 1757 nodes and has 10542 degrees-of-freedom. Shell elements were used to model floors, walls and stairs; line elements were used to model the columns and beams, and linear spring elements were used to model the rubber bearings, elastic bearings and steel dampers in the isolation layer.

Table 2.1 Results of system identification using the random excitation experiments

Mode	f_{ECCA} (Hz)	f_{N4SID} [Hz]	Error [%]	MAC	Mode Type
1	0.6533	0.6482	0.7778	0.7478	Translational
2	0.6556	0.6568	−0.1769	0.9744	Translational
3	0.7087	0.7065	0.3187	0.9854	Rotational
4	4.8563	4.8026	1.1048	0.7616	Rotational
5	5.2327	5.1258	2.043	0.9676	Rotational
6	7.4716	7.2984	2.318	0.9044	Rotational
7	10.4663	10.0556	3.9236	0.9193	Rotational
8	15.6796	16.0262	−2.211	0.9010	Rotational

3. METHODOLOGY

Although the finite element method has undergone significant advancements for modeling complex linear/nonlinear structures, obtaining an FEM that accurately represents the behavior of a real structure remains a challenging problem. Often times, the properties of an existing structure, such as those relating to its material properties or geometry, are missing or inaccurate. In the case of missing properties, assumptions must be made, but these contribute to the inaccuracies in the model [9]. For these and other reasons, FEMs undergo an updating process to reduce the discrepancies between the numerical FEM and its corresponding real structure. Over the past two decades, several methods have emerged for addressing the problem of FEM updating using a variety of techniques [10].

In this study, a modal-based approach is used for model updating, where different structural parameters are modified to match the modes shapes and frequencies of the FEM to the target mode shapes and frequencies identified from measured responses. It is assumed the equation of motion of the structure is as follows:

$$\mathbf{M\ddot{x} + C\dot{x} + Kx = f} \tag{3.1}$$

where $\mathbf{x}$ is the displacement vector of the structure relative to the ground (shake table), $\mathbf{M}$, $\mathbf{C}$ and $\mathbf{K}$ are the mass, damping and stiffness matrices, respectively, and $\mathbf{f}$ is the excitation force vector. For the undamped case, the previous equation of motion becomes:

$$\mathbf{M\ddot{x} + Kx = f} \tag{3.2}$$

This equation can be transformed into the modal space by taking the form of the generalized Eigenvalue problem, as follows:

$$\mathbf{K\Phi = \Lambda M\Phi} \tag{3.3}$$

where $\mathbf{\Phi}$ is the eigenvector matrix whose columns contain the mode shapes and $\mathbf{\Lambda}$ is a diagonal matrix whose diagonal values are the eigenvalues, i.e., the squared natural frequencies. Eq. 3.3 can be solved numerically from the FEM to obtain the mode shapes and frequencies of the structural model. The mode shapes and frequencies are often different from the target values obtained during system identification, so it is important to define metrics to evaluate the residuals between the numerical values and those computed from measurements. The residual vector $\mathbf{r}$, defined for the natural frequencies, is used to quantify the difference between computed and experimentally-determined frequencies:

$$\mathbf{r = f_m - f_c} \tag{3.4}$$

In Eq. 3.4, $\mathbf{f_m}$ is the vector of experimentally-determined target frequencies and $\mathbf{f_c}$ is the vector of computed frequencies (obtained from the eigenvalues). The Modal Assurance Criteria (MAC) [11] is used to quantify the correlation between mode shapes obtained from the FEM (φ_c) and those obtained during system identification (φ_m) as follows:

$$MAC(\varphi_m, \varphi_c) = \frac{|\varphi_m^* \cdot \varphi_c|}{\sqrt{(\varphi_m^* \cdot \varphi_m)(\varphi_c^* \cdot \varphi_c)}} \tag{3.5}$$

For the purpose of FEM updating, an objective function based on residuals in frequencies and the MAC values

can be defined for a vector of parameters $\mathbf{p}_i$ as follows:

$$J(\mathbf{p}_i) = \mathbf{r}_i^T \mathbf{W}_f \mathbf{r}_i + \mathbf{m}_i^T \mathbf{W}_m \mathbf{m}_i \tag{3.6}$$

where $\mathbf{r}_i$ is the residual in frequencies when the parameter vector $\mathbf{p}_i$ is used in the FEM. $\mathbf{W}_f$ is a diagonal weighting matrix that can specify different weights for the frequency residual values in different modes. $\mathbf{m}_i$ is a vector whose elements are $1 - \text{MAC}$ values, i.e., $\mathbf{m}_i = \left[1 - \text{MAC}(\varphi_{m1}, \varphi_{c1}^i), 1 - \text{MAC}(\varphi_{m2}, \varphi_{c2}^i), \ldots\right]$ where φ_{cj}^i is the jth computed mode from the FEM when the parameter vector $\mathbf{p}_i$ is used. $\mathbf{W}_m$ is a diagonal matrix that is used to assign different weights for matching each mode shape.

3.1. Nelder-Mead Simplex Method

In this study, the Nelder-Mead Simplex method [12] is used to solve the optimization problem involved in the FEM updating procedure. The method is implemented using MATLAB's Optimization Toolbox [13] that utilizes the algorithm developed by Lagarias *et al.* [14]. The method is one of the most popular direct optimization techniques that does not require the computation of gradients. The main procedure of the method can be summarized as follows:

1. Generate an initial simplex with $n + 1$ vertices ($\mathbf{p}_i$), where n is the dimension of the search space. For the purpose of model updating, $\mathbf{p}_i$ is the vector of parameters that are being updated.
2. Compute the objective function at each vertex of the initial simplex.
3. Generate a new point by reflecting about the midpoint of the simplex the point with highest function value.
4. Evaluate the objective function at the reflected point.
5. Change the simplex vertices' coordinates using reflection, expansion or contraction operators, depending on how the function value at the reflected point compares to the function values at the simplex vertices.
6. Iterate through steps 3–5 until a specified maximum number of iterations is performed or convergence is achieved. Typically, convergence is achieved when the function values at the vertices reach a specified tolerance or the size of the simplex is reduced below a specified threshold.
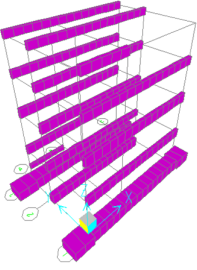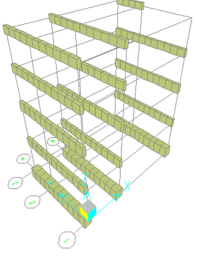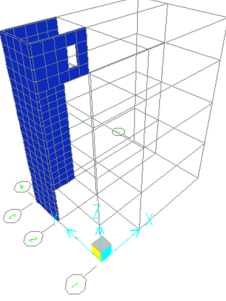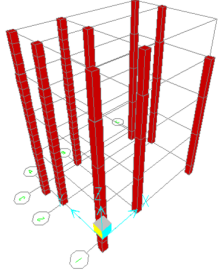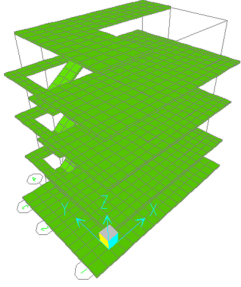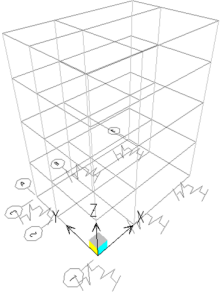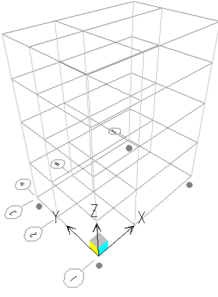
3.2. Model Updating Parameters

The process of selecting the updating parameters is a very important step in the model updating procedure. In many cases, this is done based on engineering judgment as well as geometric and computational considerations. It is important to note that, in many cases, the parameters selected for updating will end up assuming non-realistic or non-physical values [10], e.g., extremely large/small stiffness, negative stiffness or negative mass. This can be attributed to different sources of errors in the measurements, identification and idealizations in the FEM, which manifest themselves in producing non-physical parameter values. A proper choice of parameters may help reduce this drawback. After examining different sets of parameters, the final set of 21 parameters, summarized in Table 3.2, were chosen.

Using the measurements of forces in the bearings and steel dampers, along with the displacements of the isolation layer, the force-displacement curves can be obtained for the isolators (shown in Figure 3.1). The curves show behaviors that are dominated by a linear relationship, so linear regression was used to obtain proper initial values for these parameters. The fitted isolation stiffness values are summarized in Table 3.1. The initial values for the masses were chosen to be zero, while the initial values for the modulus of elasticity for the different structural elements were chosen based on the formula provided by the ACI building code requirements for structural concrete [15].

Table 3.1 Effective stiffness of isolators obtained from linear regression of the force-displacement curves

Steel Dampers	Rubber Bearings	Slide Bearings
4621 kN/m	1050 kN/m	1570 kN/m

Table 3.2 Parameters chosen for model updating

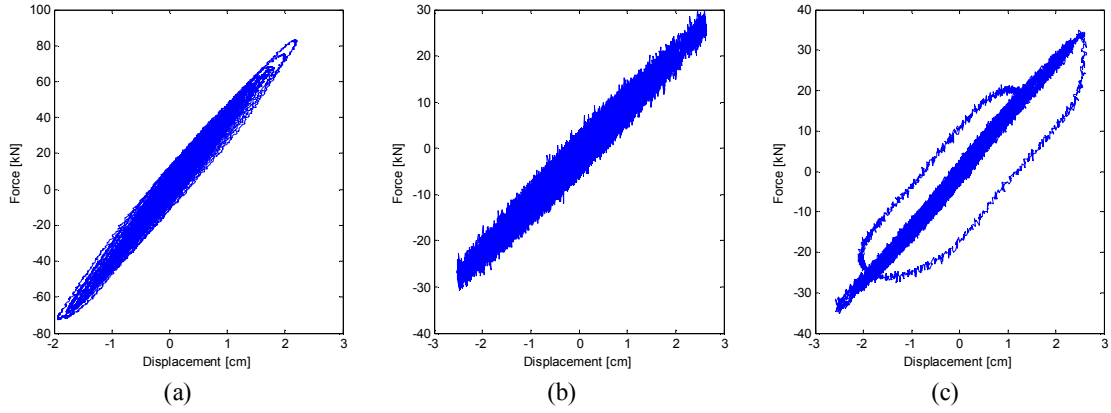| Parameters	Locations	Parameters	Locations
E_{bx} : Young's modulus of Beams in the X direction		E_{by} : Young's modulus of Beams in the Y direction	
E_w : Young's modulus of Walls		E_c : Young's modulus of Columns	
E_s : Young's modulus of slabs		$K_{sdx1}/K_{sdy1}/K_{sdx2}/K_{sdy2}$: Stiffnesses of the two steel dampers in X and Y directions, respectively. $K_{rbx1}/K_{rby1}/K_{rbx2}/K_{rby2}$: Stiffnesses of the two rubber bearings in X and Y directions, respectively. $K_{sbx1}/K_{sby1}/K_{sbx2}/K_{sby2}$: Stiffnesses of the two slide bearings in X and Y directions, respectively.	
$m_1/m_2/m_3/m_4$: Four additional masses added at the isolation level. These masses were added to allow for correcting the mass distribution if it is different in the model from the real structure.			

Figure 3.1 Force-Displacement curves of the isolators: (a) Steel Dampers; (b) Rubber Bearings; (c) Sliding Bearings

4. RESULTS AND DISCUSSION

The match between modal parameters obtained from the FEM and those identified from measurements must be examined prior to performing the model updating, as shown in Figure 4.1(a) for the first 6 modes. It is obvious from the figure that the frequencies of the first 3 modes correlate well, even before updating the model; this may be attributed to the fact that the initial values used for parameters that represent the isolation layer (bearings and dampers stiffnesses) were obtained from the experimental results. It was also found that the first 3 modes are ones in which the dominant motion is the rigid movement of the super-structure above the isolation layer, which means that those modes are highly dependent on the isolation layer properties and less dependent on the superstructure properties. It can also be noted that mode shapes 3 and 6 are well paired; for instance, mode 6 in the FEM has strong correlation with the 6th identified mode, but it is not strongly correlated to any other identified mode and vice versa. On the other hand, modes shapes 1, 2, 4 and 5 are not well paired. For the first two modes, this might be attributed to the fact that these two modes are coupled; however, the same argument cannot be made for modes 4 and 5.

The Nelder-Mead Simplex method was used to update the selected 21 parameters. The weight matrix in the 1st term of the cost function is selected to be $\mathbf{W}_f = c \times [\text{diag}(\mathbf{f}_m)]^{-2}$, which normalizes the error in frequency by dividing it by the target frequency. The factor c is used to scale the first term in the cost function so it has similar magnitude to the second term for the first few iterations. The weighting matrix of the second term is an identity matrix, which assigns identical weight on each mode shape match.
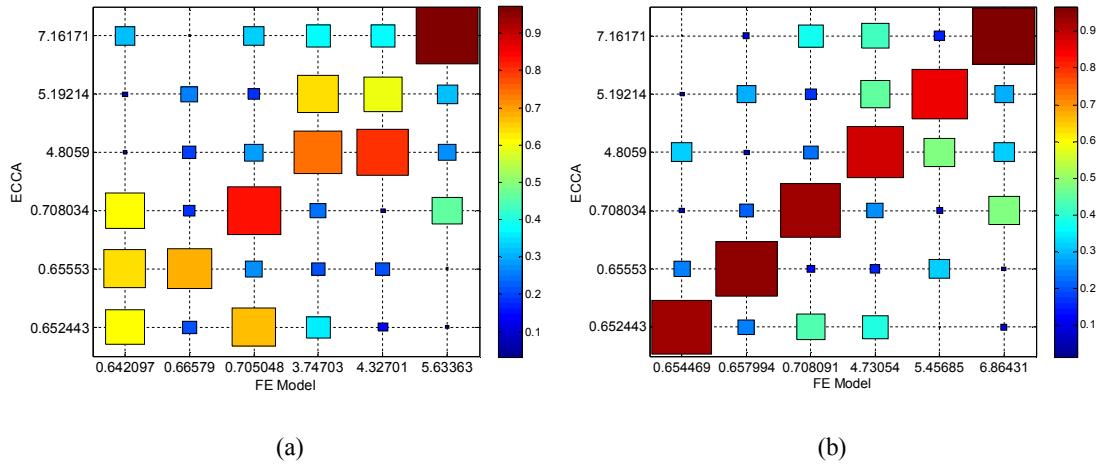

Figure 4.1 Match between the FEM and the identified modes: (a) Initial FEM; (b) Updated FEM
(values on the axes are frequencies in Hz)

The optimization procedure was carried out for 500 iterations; the resulting convergence in the cost function is shown in Figure 4.2. The updated FEM matches well with identified mode shapes and frequency as shown in Figure 4.1(b). Table 4.1 compares the frequencies and MAC values of the model before and after updating. It is important to note that the first 3 modes in the updated model correlate better with the identified values compared to last 3 modes. This can be shown by looking at both the MAC values and also the errors in frequencies, which is lower by one order of magnitude for the first 3 modes. This can be attributed to the chosen weighting matrices and/or the fact that the first 3 modes are highly dependent on the parameters in the isolation layer, whose initial values were obtained from fitting the experimental results. In a future study, different weighting might be investigated to achieve a better match for the last 3 modes, in addition to introducing additional parameters to update the masses in the superstructure.
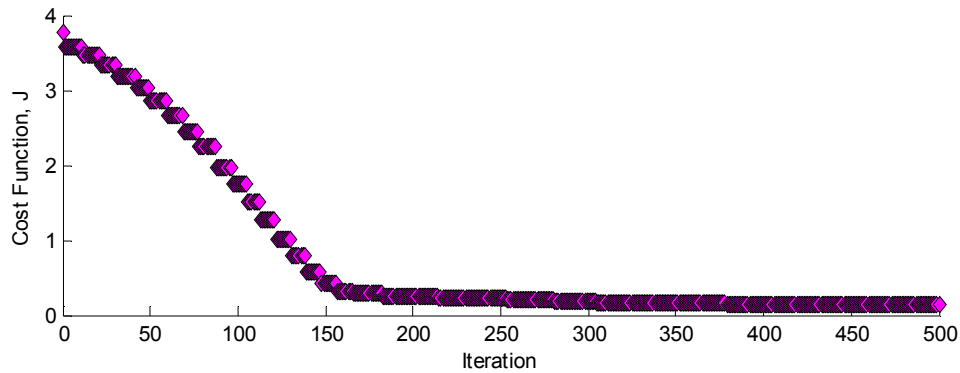

Figure 4.2 Minimization of cost function value in 500 iterations

Table 4.1 Frequency and mode shape comparison between the model before and after the updating

Mode	Identified Frequency	Initial FEM		Updated FEM	
		Frequency [Hz] (error [%])	MAC	Frequency [Hz] (error [%])	MAC
1	0.6524	0.6421 (1.57)	0.4924	0.6545 (–0.32)	0.9295
2	0.6555	0.6658 (–1.57)	0.6744	0.6580 (–0.38)	0.9487
3	0.7080	0.7050 (0.42)	0.7729	0.7081 (–0.01)	0.9271
4	4.8059	3.7470 (22.03)	0.7355	4.7305 (1.57)	0.8782
5	5.1921	4.3270 (16.66)	0.5873	5.4569 (–5.10)	0.8618
6	7.1617	5.6336 (21.34)	0.9552	6.8643 (4.15)	0.9669

It is also important to note that the final values of the updated moduli of elasticity were all increased noticeably during the model updating, leading to a stiffer model, with very significant increases for the beams and columns. Compared to the initial assigned values, E_{bx} increased by 104%, E_{by} increased by 28%, E_c increased by 71%, E_s increased by 12% and E_w increased by 10%. The significant increase in the beams elasticity moduli may be attributed to the effect of beam offset from the floor, as projected RC beams often behave as a T-shaped section (including adjacent zones from the slab), which results in a significantly higher stiffness compared to that of a rectangular section. The increase in elasticity moduli of the columns and walls may be resulting from the contribution of the non-structural walls. In many cases, non-structural elements can lead to increase in the vertical stiffness as well as the lateral stiffness of the structure as they provide additional coupling between other lateral loads resisting elements such as the moment frames and the structural walls. On the other hand, the masses have only slightly increased to result in a total additional mass of 18.2 tons, merely a 2.5% increase in the total mass of the structure. Though, it has to be noted that the additional masses were not distributed uniformly on the 4 locations chosen in the isolation layer, but rather have opposite signs on opposite sides of the building, leading to a slight shift in the center of mass of the FEM.

5. CONCLUSIONS

In this study, a FEM was developed for the four-story base-isolated building that was tested at the E-defense facility in 2013. The FEM was updated using the Nelder-Mead Simplex method to match the identified modes and frequencies obtained from system identification. The FEM updating procedure showed a good convergence in terms of minimization of the cost function and the updated model shows good agreement with the experimental

results. The first 3 modes show stronger correlation with the experimental results compared to the last 3 modes, which is probably a result of the chosen weighting matrices and the set of optimization parameters. The updated model is significantly stiffer compared to the initial model, as evidenced by the significant increase in the moduli of elasticity of all the structural elements; on the other hand, only a slight increase of mass was observed. Future studies may investigate obtaining a stronger correlation for the last 3 modes by introducing more optimization parameters in the superstructure and investigating the use of different weighting matrices in the optimization procedure.

ACKNOWLEDGEMENT

REFERENCES

1. Ma, X., Eatherton, M., Hajjar, J., Krawinkler, H., and Deierlein, G. (2010). Seismic Design and Behavior of Steel Frames with Controlled Rocking—Part II: Large Scale Shake Table Testing and System Collapse Analysis. *Proceedings of Structures Congress*. Orlando, FL, USA.
2. Deierlein, G., Krawinkler, H., Ma, X., Eatherton, M., Hajjar, J., Takeuchi, T., Kasai, K., and Midorikawa, M. (2011). Earthquake Resilient Steel Braced Frames with Controlled Rocking and Energy Dissipating Fuses. *Steel Construction*, **4**:**3**, 171–175.
3. Ryan, K. L., Sato, E., Sasaki, T., Okazaki, T., Guzman, J., Dao, N., Soroushian, S., and Coria, C. (2013). Full Scale 5-Story Building with Triple Pendulum Bearings at E-Defense. *Network for Earthquake Engineering Simulation (distributor), Dataset, DOI:10.4231/D3X34MR7R*.
4. Sato, E., T. Sasaki, K. Fukuyama, K. Tahara, and K. Kajiwara. (2013). Development of Innovative Base-Isolation System Based on E-Defense Full-Scale Shake Table Experiments Part I: Outline of Project Research. *AIJ Annual Meeting*. Hokkaido, Japan (in Japanese).
5. Sato, E., and Sasaki, T. (2013). Personal Communication of Design Drawings.
6. Brewick, P., Barrios Hernandez, J., Elhaddad, W., Johnson, E., Christenson, R., Sato, E., and Sasaki, T. (2015). Modal Analysis of a Full-Scale Four-Story Reinforced-Concrete Base-Isolated Building Subjected to Random and Simulated Earthquake Shake Table Excitations. *Proceedings of the International Workshop on Structural Health Monitoring*. Presented at the International Workshop on Structural Health Monitoring, Palo Alto, CA, USA.
7. Van Overschee, P., and De Moor, B. (1994). N4SID: Subspace Algorithms for the Identification of Combined Deterministic-Stochastic Systems. *Automatica*, **30**:**1**, 75–93.
8. Hong, A., Ubertini, F., and Betti, R. (2012). New Stochastic Subspace Approach for System Identification and Its Application to Long-Span Bridges. *Journal of Engineering Mechanics*, **139**:**6**, 724–736.
9. Mottershead, J. E., Link, M., and Friswell, M. I. (2011). The Sensitivity Method in Finite Element Model Updating: A Tutorial. *Mechanical Systems and Signal Processing*, **25**:**7**, 2275–2296.
10. Mottershead, J. E., and Friswell, M. I. (1993). Model Updating in Structural Dynamics: A Survey. *Journal of Sound and Vibration*, **167**:**2**, 347–375.
11. Allemang, R. J., and Brown, D. L. (1982). A Correlation Coefficient for Modal Vector Analysis. *Proceedings of 1st International Modal Analysis Conference, Orlando, FL*.
12. Nelder, J. A., and Mead, R. (1965). A Simplex Method for Function Minimization. *The Computer Journal*, **7**:**4**, 308–313.
13. *MATLAB and Optimization Toolbox Release 2013b*. (2015). Natick, Massachusetts, United States: The MathWorks, Inc.
14. Lagarias, J. C., Reeds, J. A., Wright, M. H., and Wright, P. E. (1998). Convergence Properties of the Nelder-Mead Simplex Method in Low Dimensions. *SIAM Journal of Optimization*, **9**, 112–147.
15. American Concrete Institute. (2014). Building Code Requirements for Structural Concrete (318-14) and Commentary (318R-14).